Bioorganic & Medicinal Chemistry 22 (2014) 6953–6960

Contents lists available at ScienceDirect

Bioorganic & Medicinal Chemistry

journal homepage: www.elsevier.com/locate/bmc

Synthesis and biological evaluation of novel oxindole-based RTK inhibitors as anti-cancer agents

Gaozhi Chen [†], Qiaoyou Weng [†], Lili Fu, Zhe Wang, Pengtian Yu, Zhiguo Liu, Xiaokun Li, Huajie Zhang [*], Guang Liang [*]

Chemical Biology Research Center, School of Pharmaceutical Sciences, Wenzhou Medical University, Wenzhou, Zhejiang 325035, China

ARTICLE INFO

Article history:
Received 27 July 2014
Revised 13 October 2014
Accepted 14 October 2014
Available online 29 October 2014

Keywords:
Anticancer drug
Chemical synthesis
Drug design
Oxindole
Receptor tyrosine kinase inhibitor

ABSTRACT

Given that receptor tyrosine kinases (RTKs) have emerged as key regulators of all aspects of cancer development, including proliferation, invasion, angiogenesis and metastasis, the RTK family represents an important therapeutic target for anti-cancer drug development. Oxindole structure has been used in RTK inhibitors such as SU4984 and intedanib. In this study, two series of new heterocyclic compounds containing oxindole scaffold have been designed and synthesized, and their inhibitory activity against the proliferation of nine cancer cell lines has been evaluated. Among them, compounds **9a** and **9b** displayed the strongest anti-proliferative activity with the IC_{50}s below 10 μM. Flow cytometric analysis showed that the compounds **9a** and **9b** dose-dependently arrested the cell cycle at G0/G1 phase. Although the leading compounds SU4984 and intedanib targets FGFR1, the kinase activity test revealed that these compounds only showed slight inhibitory activity on FGFR1 kinase. Further enzymatic test aided by molecular docking simulation in the ATP-binding site demonstrated that **9a** and **9b** are potent inhibitors of c-Kit kinase. These compounds are worthy of further evaluation as anticancer agents.

1. Introduction

Cancer is continuing to harm human health both in developed and developing countries.[1–2] Surpassing heart disease, it has become the worldwide number one killer. Several anticancer agents, such as indomethacin,[3] taxol,[4] 5-fluorouracil,[5] vinblastine,[6] camptothecin and its derivatives (topotecan and irinotecan),[7] etoposide[8] and mitoxantrone[9–10] are used clinically around the world. However, the usage of these drugs has been linked with various side effects, such as bone marrow suppression, gastrointestinal toxicity, low blood pressure, hair loss and constipation. Therefore, new chemical entities for the effective and safe cure of cancer are still an active area of research in the scientific community.

Protein kinases are critical components of cellular signal transduction cascades. They form one of the most important target classes in drug development, as they are directly involved in many diseases, including cancer.[11–12] Therefore, small molecule kinase inhibitors have been successfully introduced to the drug market as a selective anticancer agents with few side effects.[13–14] To date, the FDA has approved ten protein kinase inhibitors as drugs for the treatment of different types of cancer, including both solid and non-solid tumors.[15] Over 300 kinase inhibitors are currently in clinical development, and many more are at the preclinical study stage of development. The vast majority of these compounds are reported to target the kinase ATP binding site, and more than 500 protein kinases identified in the human genome have an ATP binding site.[16] Small molecule kinase inhibitors achieve their inhibitory activity against kinases by thoroughly mimicking the binding mode of the ATP molecule. Therefore, the design of small molecule kinase inhibitors based on the characteristics of the ATP binding site is a rational approach to the discovery of anti-cancer agents.

Fibroblast growth-factor receptors (FGFRs) form a sub-family of the receptor tyrosine kinase (RTK) superfamily, and are encoded by four genes, FGFR1, FGFR2, FGFR3, and FGFR4. FGFRs are involved in the regulation of cell proliferation and migration, angiogenesis, organ development and other processes. Studies have confirmed that the activation and overexpression of FGFR results in carcinogenic functions in cells, including excessive proliferation and the prevention of apoptosis, and are found to be closely related to the development and progression of tumors in humans.[17–18] Considering the prominent role of FGFRs in cancer development, it would be desirable to develop potent FGFR inhibitors.

Oxindole-based chemical scaffolds have been broadly used as protein kinase inhibitors because oxindoles generally form

* Corresponding authors. Tel.: +86 13868888091 (H.Z.); tel./fax: +86 577 86699396 (G.L.).
E-mail addresses: HuajieZhang2014@163.com (H. Zhang), wzmcliangguang@163.com (G. Liang).
† These authors contribute equally to this work.

http://dx.doi.org/10.1016/j.bmc.2014.10.017
0968-0896/

hydrogen bonds with the backbone of the hinge segment of the kinase ATP binding domain.[19] For instance, intedanib[20] acts as a triple kinase inhibitor with inhibitory activity against VEGFR, FGFR and PDGFR kinases, resulting in suppressed vascularization and proliferation of tumor tissues causing starvation and death of tumor cells. SU6668[21] is a another triple kinase inhibitor of VEGFR, FGFR and PDGFR kinases and SU4984 was reported to inhibit FGFR1 specifically in 1997[22] with a moderate IC_{50} of 10–20 μM. Inspired by the potential inhibitory ability, an oxindole scaffold has been chosen for further structural modification.

The ATP binding pocket of kinase is located in the cleft between the N- and C-lobes of the kinase, and is composed of residues from the N- and C-lobes, the nucleotide-binding loop, and the hinge region that connects the two lobes.[17] Common pharmacophores of oxindole-based kinase inhibitors usually divided into three main categories. First, the oxindole of the inhibitors forms a hydrogen bond with two residues from the hinge region and binds in a similar fashion to the ATP's purine ring (this part is denoted by a red rectangle in Fig. 1). Second, the methylpyrrole of SU6668 and the 3-phenyl ring of SU4984 and Intedanib form van der Waals interactions with hydrophobic groups present in a hydrophobic pocket located outside of the ATP binding pocket (the hydrophobic groups of compounds are marked by a blue rectangle in Fig. 1). The third feature is a nucleotide-binding domain which is located adjacent to the hydrophobic domain. The long-chain carboxyl group of SU6668 and the piperazinecarboxylate moiety of SU4984 and intedanib form a hydrogen bond with the amino acid residue in the nucleotide-binding domain (this part is marked by green ovals in Fig. 1).[17]

Two series of indolin-2-one were designed based on the structure of SU4984 and the structural features of the ATP-binding domain, and three pharmacophores were modified according to the mechanisms of interaction between the group and ATP binding site in order to determine the most effective kinase inhibitor with the greatest affinity for the ATP binding site. The main difference between two series compound is the linker between the oxindole and the hydrophobic groups.

2. Material and methods

2.1. Chemical synthesis

2.1.1. General information

Solvents were distilled under the positive pressure of dry argon before use and dried using standard methods. Acetonitrile (MeCN) and Tetrahydrofuran (THF) were distilled over calcium hydride and stored over 4A molecular sieves. All starting materials and reagents were commercially available. Unless otherwise noted, chemicals were obtained from local suppliers and were used without further purification. All reactions were monitored by thin-layer chromatography (silica gel 60 F254 glass plates). NMR spectra were recorded on Bruker 600 MHz instruments, and the chemical shifts were presented in terms of parts per million with TMS as the internal reference. Electron-spray ionization mass spectra in positive mode (ESI-MS) data were obtained with a Bruker Esquire 3000+ spectrometer. Column chromatography purifications were carried out on Silica Gel 60 (E. Merck, 70–230 mesh).

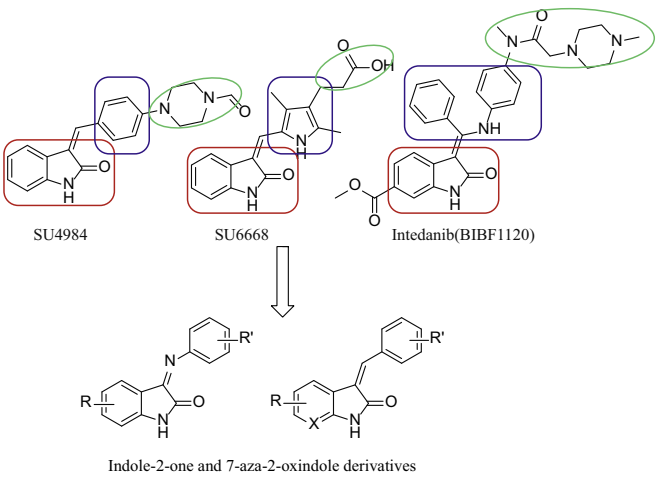

Figure 1. Structural skeleton and chemical structures of Oxindole-based protein kinase inhibitors and the designed compound in this paper.

2.1.2. General procedure for the synthesis of compounds 1a–1g, 2a, 3a

Various aldehydes (1.0 equiv) were added to stirred solutions of indolin-2-one, 5-chloroindolin-2-one or 7-azaoxindole (1.0 equiv) in absolute ethanol. After stirring at room temperature for 5 min NaOEt/EtOH (0.5 mL) was added and the mixture was then stirred at room temperature overnight. The solvent was then removed under vacuum. The residue was washed with saturated sodium chloride solution and then extracted with ethyl acetate. The organic layer was dried over anhydrous magnesium sulfate and concentrated under vacuum. The solid part was purified by chromatography over silica gel using ethyl acetate/petroleum ether as the eluent to afford desired compounds **1a**–**1g**, **2a**, **3a**.

2.1.3. Synthesis of intermediate 4

A reaction mixture of 4-fluorobenzaldehyde (1.0 equiv) and piperazine (3.0 equiv) in 2-methoxyethanol was stirred at 110 °C for 3–5 h. The solvent was then removed under vacuum. The residue was washed with saturated sodium chloride solution and filtrated. The solid part was purified by chromatography over silica gel using ethyl acetate/methanol as the eluent to generate intermediate **4**.

2.1.4. Synthesis of Intermediates 5 and 6

Intermediate 4 (1.0 equiv) was added to a stirred solution of indolin-2-one or 7-azaoxindole (1.0 equiv) in absolute ethanol. After stirring at room temperature for 5 min, NaOEt/EtOH (0.5 mL) was added, and then the mixture was stirred at room temperature overnight. The solvent was then removed under vacuum. The residue was washed with saturated sodium chloride solution and filtrated. The solid part was purified by chromatography over silica gel using ethyl acetate/methanol as the eluent to generate intermediates **5** and **6**.

2.1.5. Synthesis of compounds 7a and 8a

A reaction mixture of intermediate **5** or **6** in ethyl formate was stirred at 50 °C overnight. The solvent was then removed under vacuum. The residue was purified by chromatography over silica gel using ethyl acetate/petroleum ether as the eluent to afford desired compounds **7a** and **8a**.

2.1.6. General procedure for the synthesis of compounds 9a–9c and 10a–10c

Acryloyl chloride, 3-chloropropionyl chloride or Benzoyl chloride (1.1 equiv) was added to a stirred solution of intermediate **5** or **6** (1.0 equiv) in Tetrahydrofuran (THF). After stirring at room temperature for 5 min, Et_3N (0.5 mL) was added and the mixture was then stirred at room temperature for 2–4 h. The solvent was then removed under vacuum. The residue was washed with saturated sodium chloride solution and then extracted with ethyl acetate. The organic layer was dried over anhydrous magnesium sulfate and concentrated under vacuum. The solid was purified by chromatography over silica gel using ethyl acetate/petroleum ether as the eluent to afford desired compounds **9a**–**9c**, **10a**–**10c**.

2.1.7. Synthesis of intermediates 11

A reaction mixture of 6-chloro-3-nitropyridin-2-amine (1.0 equiv), morpholine (1.0 equiv) and K_2CO_3 (3.0 equiv) in MeCN was stirred at 80 °C for 3–5 h. The mixture was extracted with CH_2Cl_2 and the organic layer washed with brine, dried over anhydrous magnesium sulfate, and concentrated under vacuum. The solid part was purified by chromatography over silica gel using ethyl acetate/petroleum ether to generate intermediate **11**.

2.1.8. Synthesis of intermediates 13

A reaction mixture of 3-chloro-4-nitrobenzoic acid (1.0 equiv) and H_2SO_4 in absolute ethanol was stirred at 80 °C for 3–5 h. The mixture was extracted with ethyl acetate and the organic layer washed with brine, dried over anhydrous magnesium sulfate, and concentrated under vacuum. The solid part was purified by chromatography over silica gel using ethyl acetate/petroleum ether to generate intermediate **13**.

2.1.9. Synthesis of intermediates 14 and 17

A reaction mixture of intermediate **13** (1.0 equiv), morpholine or 3,5-dimethoxyaniline (1.0 equiv) and K_2CO_3 (3.0 equiv) in MeCN was stirred at 80 °C for 3–5 h. The mixture was extracted with CH_2Cl_2 and the organic layer washed with brine, dried over anhydrous magnesium sulfate, and concentrated under vacuum. The solid part was purified by chromatography over silica gel using ethyl acetate/petroleum ether to generate intermediate **14** and **17**.

2.1.10. Synthesis of intermediates 16

A solution of the intermediate **14** (1.0 equiv) in absolute ethanol was added to a solution of 20% NaOH and stirred at 80 °C for 3–5 h. The ethanol was then removed under vacuum. The HCl (aq) was dropped into the residual solution until the pH of the solution was equal to 7. The solid part was filtered to generate intermediate **16**.

2.1.11. Synthesis of intermediates 12, 15 and 18

Sodium dithionite (3 equiv) was added to a solution of intermediate **11**, **14** or **17** (1.0 equiv) in a mixture of ethanol (20 mL) and water (4 mL). The reaction mixture was refluxed at 90 °C for 2–3 h then cooled to room temperature. The reaction mixture was diluted with water (40 mL) and then extracted with ethyl acetate. The combined organic layers were washed with brine, dried over anhydrous magnesium sulfate, and concentrated under vacuum. The solid part was purified by chromatography over silica gel using ethyl acetate/petroleum ether as the eluent to generate intermediates **12**, **15** and **18**.

2.1.12. General procedure for the synthesis of intermediate 20 and compounds 19a–19l

A reaction mixture of the various substituted amines, hydrazine or intermediate **12**, **15**, **18** (1.0 equiv) and 5-chloroisatin (1.0 equiv) in methanol was stirred at 60 °C for 3–5 h. The solvent was then removed under vacuum. The residue was washed with saturated sodium chloride solution and filtrated. The solid was purified by chromatography over silica gel using ethyl acetate/petroleum ether as the eluent to afford intermediate **20** and desired compounds **19a**–**19l**.

2.1.13. Synthesis of compounds 21a and 21b

A reaction mixture of EDC·HCl (1.1 equiv) and HOBt (1.3 equiv) was stirred with intermediate **16** or furan-2-carboxylic acid (1.0 equiv) at 0–8 °C in CH_2Cl_2. After 10 min, intermediate **20** was added, and the mixture was stirred at 0–8 °C for 1 h before being stirred at room temperature overnight. The residue was washed with saturated $NaHCO_3$ solution and extracted with CH_2Cl_2. After solvent evaporation, the solid was purified by chromatography over silica gel using ethyl acetate/petroleum ether as the eluent to afford desired compounds **21a** and **21b**.

The spectral data of new or unreported compounds are shown in Supplementary materials.

2.2. Cell lines

All the cell lines including Human lung adenocarcinoma cell line H1975, Human glioma cell line U251, Human hepatoma cell line Bel7402, Human non-small cell lung cancer cell line HCC827, Human lung tumor cell lines H460, Human breast cancer cell line SK-BR-3, Human ovarian cancer cell linePM8910, Human gastric cancer cell line SGC-7901, Human non-small cell lung cancer cell line A549 and Normal rat kidney cell line NRK-52E were purchased from Cell Bank (Shanghai Institutes for Biological Sciences, CAS, Shanghai, China).

2.3. Cell proliferation assay

H1975, U251, Bel7402, HCC827, H460, SK-BR-3, PM8910, SGC-7901 and A549 cell lines (4×10^4 cells/ml) were cultured and seeded into 96-well plates. After overnight incubation, the cells were incubated with compounds at 10 μM dissolved in DMSO at 37 °C in an atmosphere of 5% CO2 for 72 h. The control samples received the same volume of DMSO. Cell viability was determined by using an MTS assay (Promega, San Luis Obispo, CA). Briefly, MTS dye solution was added and incubated in a CO_2 incubator for 4 h. Absorbance was measured by using the spectraMax M2 microplate reader (MolecularDevices, Sunnyvale, CA) at 490 nm and the results are expressed as the inhibition of cell proliferation calculated as the ratio $[(1 - (\text{OD490 treated/OD490 control})) \times 100]$ in triplicate experiments. For the determination of the IC_{50} [50% inhibition of cell proliferation], cells were incubated with **9a** and **9b** at concentrations of 30 μM, 10 μM, 3 μM, 1 μM, 0.3 μM, and 0.1 μM in separate triplicate experiments for 72 h following the protocol mentioned before.

2.4. Kinase inhibition assays

The kinase inhibitory activities were determined using a microfluidic assay (Caliper Mobility Shift Assay) that monitors the separation of a phosphorylated product from its substrate. Briefly, the enzyme, substrate, ATP and compound were mixed in a 384-well assay plate for the phosphorylation reaction. After 1 h incubation, EDTA was added to stop the reaction. The plate was read on an EZ Reader II (Caliper Life Sciences, MA). The percentage conversion of substrate into the phosphorylated product was generated automatically and the percentage inhibition was calculated relative to blank wells (containing no enzyme and 2.5% (v/v) DMSO) and total wells (containing all reagents and 2.5% (v/v) DMSO). The recombinant kinases, including FGFR1, EGFR, c-Kit, PDGFR-β, KDR, AUR-B and SGK1, were purchased from Carna (Chuo-ku, Kobe, Japan). The ATP concentration was set at the Km values of FGFR1: 262 μM, EGFR: 2.3 μM, c-Kit: 20 μM, PDGFR-β: 38 μM, KDR: 92 μM, AUR-B: 15 μM and SGK1: 38 μM. Compounds were tested in duplicate at 3 concentrations (10, 1.0, and 0.1 μM). IC_{50} was tested from 10 μM, 3-fold dilution.

2.5. Cell cycle analysis

Cell cycle distribution was determined by flow cytometric analysis of PI-stained nuclei. DNA content was determined by FACScan flow cytometer and CellQuest software (BD Biosciences, San Jose, CA). Briefly, PM8910, SGC7901 and A549 cells were seeded in 60 mm plates .In the following days, cells were treated with the desired doses of **9a** and **9b** for 24 h. Cells were washed twice with

PBS, fixed in ice-cold ethanol (75% vol/vol in water), and stained with the PI solution (25 mg/ml PI, 180 U/ml RNase, 0.15% Triton X-100, and 30 mg/ml polyethylene glycol in 4 mmol/l citrate buffer, pH 7.8; all from Sigma–Aldrich, St. Louis, MO) overnight at 4 °C.

2.6. Molecular docking simulation

All three-dimensional structures of compounds were built using the SYBYL-X suite. Energy minimizations of small molecules were performed by the Tripos force field and the Gasteiger–Hückel charge with a distance-dependent dielectric, and the Powell conjugate gradient algorithm with a convergence criterion of 0.05 kcal/(mol × Å). Molecule docking simulations of compounds with c-Kit kinase protein (PDB ID: 3G0E) were carried out with the Surflex-Dock program interfaced with SYBYL. The ligand-binding groove on c-Kit was kept rigid, whereas all torsible bonds of compounds were set free to allow flexible docking to produce more than 100 structures. Final docked conformations were clustered within the tolerance of 1 Å root-mean-square deviation.

2.7. Statistical analysis

The results were presented as means ± SEM. Student's *t*-test was employed to analyze the differences between sets of data. Statistics were performed using GraphPad Pro (GraphPad, San Diego, CA). P values less than 0.05 (p <0.05) were considered indicative of significance. All experiments were repeated at least three times.

3. Results and discussion

3.1. Chemistry

The common synthetic route and structures of compounds **1a**–**1g**, **2a** and **3a** are outlined in Scheme 1. Compounds were synthesized by the conventional refluxing ethanol-water solution of indole-2-ones and substituted benzaldehyde in basic conditions with a yield ranging from 30% to 80%. The synthesis of compounds **7a**, **8a**, **9a**–**9c** and **10a**–**10c** began with the preparation of the key intermediate 4-(piperazin-1-yl) benzaldehyde **4** from 4-fluorobenzaldehyde and piperazine in one step (Scheme 2). Indole-2-one or 7-aza-2-oxindole was refluxed with intermediate **4** in basic conditions to afford intermediate **5** or **6**. Compounds **7a** and **8a** were obtained through the general refluxing of intermediate **5** or **6** with ethyl formate, and compounds **9a**–**9c** and **10a**–**10c** were synthesized by electrophilic substitution reaction of intermediate **5** or **6** with acyl chloride under the catalytic condition of triethylamine (yield 30–50%).

For the synthesis of the amine linked indole-2-one series compounds, **19a**–**19i** and **21a**–**21b**, reasonable synthetic routes were designed as shown in Schemes 3–5. Mixed reflux of commercially available 5-chloroisatin and substituted amines in methanol were applied to produce compounds **19a**–**19f** (yield 67–83%, Scheme 3). According to Scheme 4, intermediates **12**, **15** and **18** were prepared first, in order to generate compound **19g**–**19i**. 3-chloro-4-nitrobenzoic acid was esterified by ethanol in the presence of sulfuric acid to afford compound **13**. Compound **13** and 6-chloro-3-nitropyridin-2-amine were treated with morpholine or 3,5-dimethoxyaniline with potassium carbonate in a solution of acetonitrile to provide intermediates **11**, **14** and **17**. Reduction of the nitro compounds (**11**, **14** and **17**) to the corresponding amino intermediates (**12**, **15** and **18**) was achieved using sodium dithionite in a solution of ethanol–water. Compounds **19g**–**19h** were prepared by the reaction of commercially available 5-chloroisatin and intermediates **12**, **15** or **18** with a yield of 45–75%.

For the synthesis of compounds **21a** and **21b** (Scheme 5), intermediate **16** was first produced through the hydrolysis of **14** in sodium hydroxide solution, and intermediate **20** was obtained from 5-chloroisatin and hydrazine. One-step amidation was introduced to produce compounds **21a** (56%) and **21b** (76%) using furan-2-carboxylic acid and intermediate **16** with compound **20** under the catalytic condition of EDC-HCl and HOBt. The structures of all compounds were characterized using ^{1}H NMR, ^{13}C NMR and electrospray ionization mass spectrometry (ESI-MS). Before used in biological experiments, all synthetic compounds were purified by recrystallization or silica gel column chromatography, and HPLC method was used to determine their purity (>95%).

3.2. Anti-proliferative activities assay

The in vitro anti-proliferative activities of the synthesized compounds against nine human cancer cell lines (H1975, A549, SGC7901, U251, Bel7402, HCC827, H460, PM8910 and SK-BR3) were evaluated using an MTS assay at a compound concentration of 10 μM (Table S1).

Compounds **9a** and **9b** displayed broad spectrum anti-proliferative activity against various cell lines with a mean growth inhibitions of 51.77% and 50.93%, respectively at a concentration of 10 μM. Other compounds showed low or modest activities. Based on the promising results of compounds **9a** and **9b**, these compounds were selected for five dose tests against the 7 cell lines. The half maximal (50%) inhibitory concentration (IC_{50}) of these compounds was also measured. Compound **9a** displayed cellular activity at concentrations of 6–28 μM, with a mean IC_{50} against all the cell lines of 10.7 μM. This compound inhibited six types of cancer cell with an IC_{50} of 8 μM, and showed a high IC_{50} value of 28 μM towards the normal kidney cell line, NRK-52E. Similarly, compound **9b also** exhibited potential biological activity at concentrations from 2 μM to 30 μM with a mean IC_{50} against all the cell lines at 9.7 μM. Compound **9b** inhibited six types of cancer cell with an IC_{50} of 6.8 μM, and more than 30 μM towards the normal cell line, NRK-52E. Table 1 shows the IC_{50} of compounds **9a** and **9b** against those the cell lines. These results indicate that compounds **9a** and **9b** have potential anti-proliferative activities against cancer cell lines, but low activities towards normal cells. However, the exact mechanism of action is still unknown.

3.3. Enzyme activity inhibition assay

In order to evaluate the activity of our designed compounds as kinase inhibitors, kinase inhibition assay was carried out using the

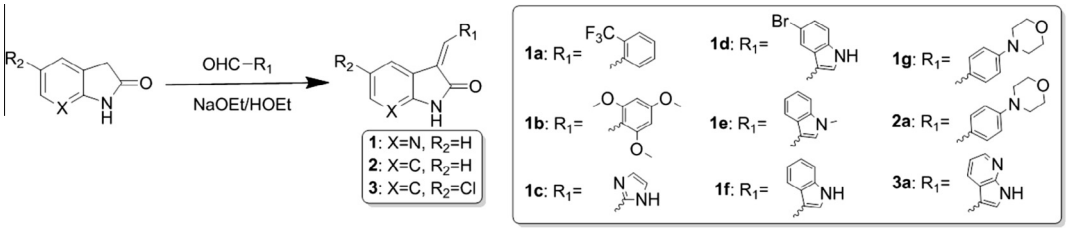

Scheme 1. Synthetic pathway for the new indole-2-ones and 7-aza-2-oxindoles **1a**–**1g**, **2a**, **3a**.

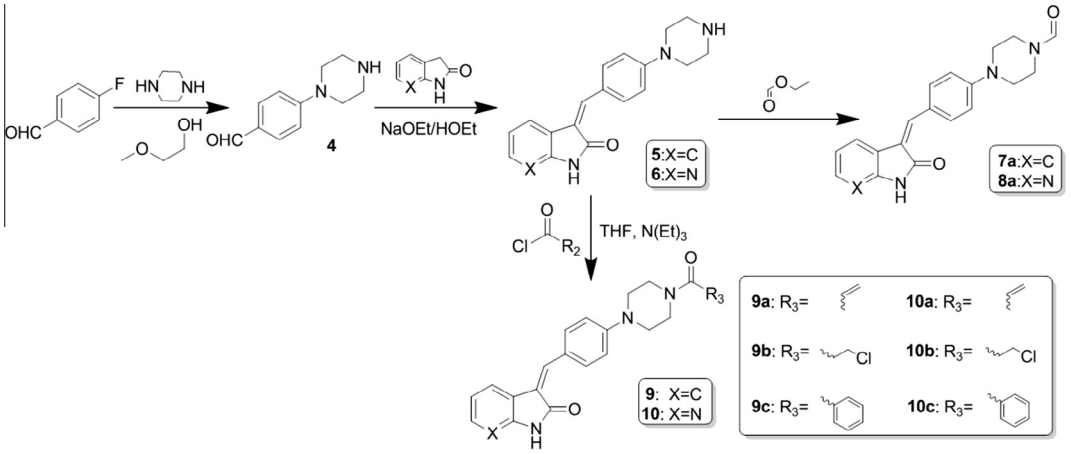

Scheme 2. Synthetic route for the new indole-2-ones and 7-aza-2-oxindoles **7a**, **8a**, **9a–9c**, **10a–10c**.

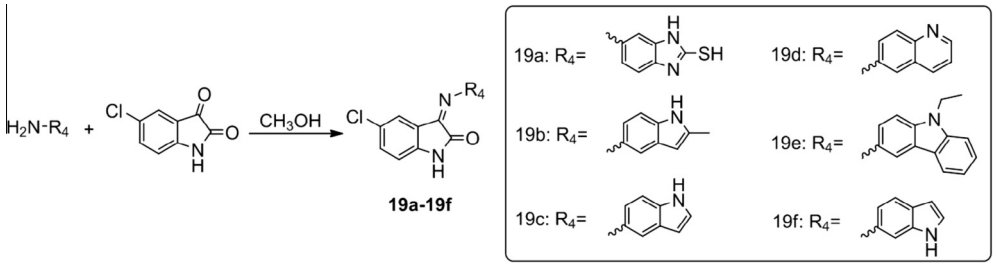

Scheme 3. Synthetic step for the new amine linked indole-2-ones **19a–19f**.

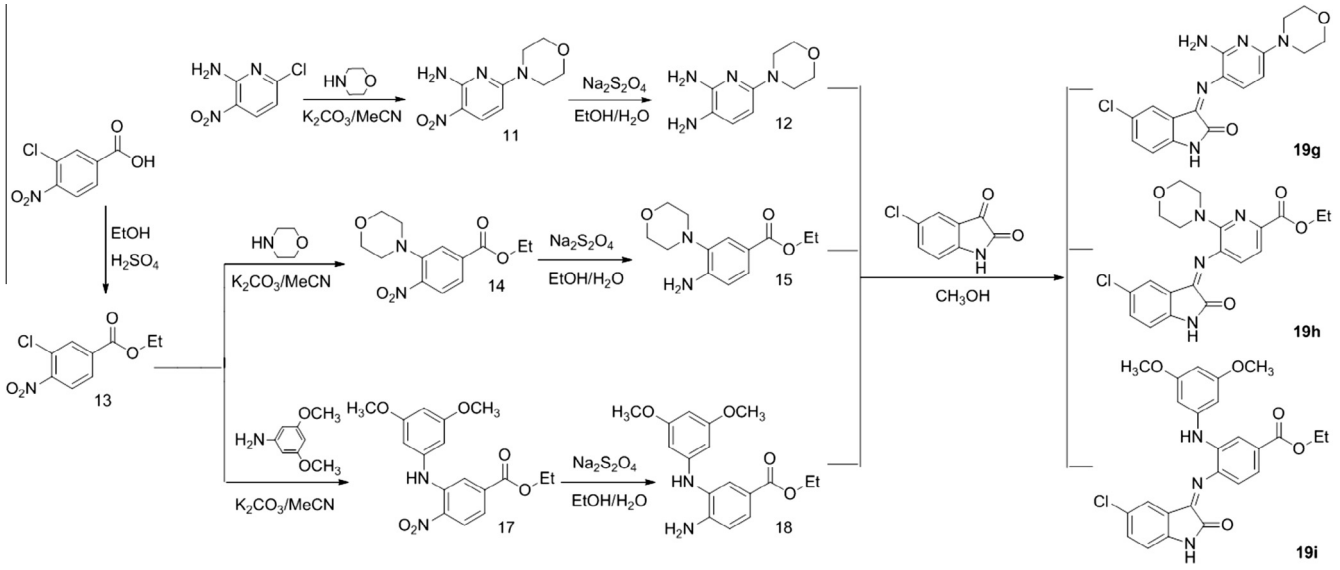

Scheme 4. Synthetic milestone for the new amine linked indole-2-ones **19g–19i**.

Caliper Mobility Shift Assay. The percentage inhibition of FGFR1 tyrosine kinase enzymatic activity caused by our compounds was evaluated against a reference kinase inhibitor, staurosporine, at an IC_{50} of 9.7 nM. Unfortunately, the compounds showed weak to moderate inhibitory activity against the FGFR1 kinase, as shown in Table 2. It is noteworthy that compound **7a**, which exhibited the highest inhibition of FGFR1 shared the same structure with the FGFR1inhibitor named SU4984. These data imply that the cellular activity of active compounds was not due to the inhibition of FGFR1.

Compounds **9a** and **9b** showed excellent cellular activity against the tested cancer cell lines. Since **9a** and **9b** showed low inhibition of FGFR1, they were tested against five other kinases at a dose of 0.1, 1, and 10 μM (Table 3). We selected these kinases from different kinase families whose inhibitors share some structural similarities with our lead compound, Intedanib. This assay was used to determine whether compounds **9a** and **9b** have an unanticipated target activity that may be responsible for their high cellular anti-proliferative activity. Compounds **9a** and **9b** showed a superior inhibitory activity against Aurora B kinase at 10 μM but

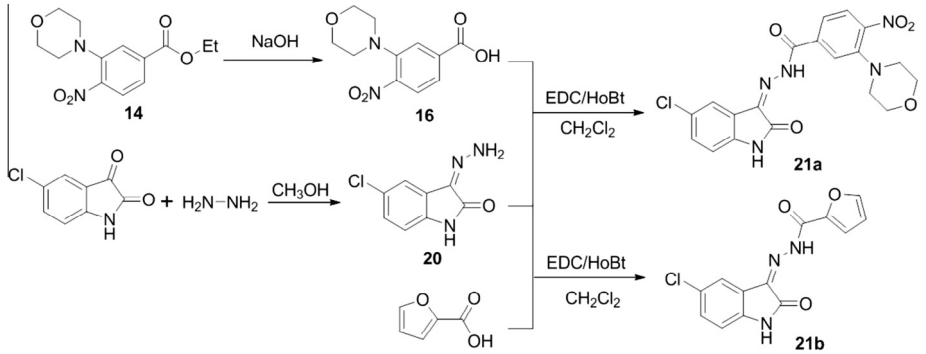

Scheme 5. Synthetic milestone for the new amine linked indole-2-ones **21a**–**21b**.

Table 1
MTS testing results of compound 9a and 9b against representative cell lines

Cell name	Compound (IC_{50}, μM)	
	9a	**9b**
PM8910	6.74 ± 0.15	2.76 ± 2.83
HCC827	7.00 ± 0.98	12.66 ± 1.4
SGC7901	9.75 ± 0.49	2.85 ± 0.21
Bel7402	7.68 ± 0.32	3.39 ± 4.13
A549	10.13 ± 0.28	3.04 ± 0.18
H460	11.50 ± 1.65	20.05 ± 13.67
NRK-52E	28.78 ± 0.68	>30

Table 2
Enzyme inhibition assay of the synthesized compounds against FGFR1 at 10 μM

Compound	% Inhibition of FGFR1 at 10 μM	Compound	% Inhibition of FGFR1 at 10 μM
1a	53.2	**10a**	22.24
1b	38.4	**10b**	30.3
1c	6.7	**10c**	49.3
1d	10.9	**19a**	−28.85
1e	6.4	**19b**	4.8
1f	3.11	**19c**	9.3
1g	16.6	**19d**	0.58
2a	46.0	**19e**	0.36
3a	8.1	**19f**	21.8
7a	72.5	**19g**	16.6
8a	49.1	**19h**	−14.8
9a	48.2	**19i**	−1.42
9b	47.4	**21a**	−16.8
9c	65.0	**21b**	11.4

showed highest inhibitory effects on c-Kit at lower concentration. The IC_{50} of two compounds towards Aur B and c-Kit were further determined. The result shows that **9a** and **9b** inhibit Aur B kinase at the IC_{50} of 2205 nM and 587 nM, while inhibit c-Kit kinase with the IC_{50} of 128 nM and 71 nM, respectively (Table 4). Thus, **9a** and **9b** showed about 10-fold stronger inhibition against c-Kit than Aur B and exhibited modest results on the other tested kinases. C-Kit kinase is one of the receptor tyrosine kinase which can activates the mitogen-activated protein kinases (MAPKs) and phosphoinositide-3-kinase(PI3 K) pathway and regulates the gene expression, cell growth, proliferation and differentiation.[23–24] Both the expression level and the kinase activity of c-Kit kinases were found to be up-regulated in many human cancers, suggesting a role for use of pharmacologic inhibitors of c-kit in the treatment of c-Kit-dependent malignancies.[25–26] There are many compounds that target c-Kit kinase that are now in different stages of clinical testing for the treatment of many types of tumors.[27–28] Fortunately, it was reasonable for **9a** and **9b** to have inhibitory activity on the c-Kit enzyme as they were designed based on the

Table 3
Inhibition rates of compound **9a** and **9b** against some kinases

Kinase	% Inhibition of compd **9a** (μM)			% Inhibition of compd **9b** (μM)		
	10	1	0.1	10	1	0.1
c-Kit	88.2	55.3	19.1	57.6	56.4	31.9
PDGFRb	61.8	26.2	0.4	76.0	46.7	13.6
KDR	30.6	7.2	13.4	62.6	14.7	6.0
Aur B	93.5	41.6	4.5	88.3	53.5	14.4
SGK1	90.7	38.3	2.2	42.4	11.8	3.56
EGFR	75.4	30.1	14.9	24.3	20.0	19.1

Table 4
IC_{50} of compounds **9a** and **9b** against Aur B and c-Kit

Kinase	IC_{50} of **9a** (nM)	IC_{50} of **9b** (nM)
c-Kit	128	71
Aur B	2205	587

indolinone scaffold, and many c-Kit inhibitors are indolinone based compounds.[29] The high inhibitory activity exhibited by compounds **9a** and **9b** on c-Kit kinase may explain their excellent antiproliferative profiles against the tested cancer cell lines.

3.4. Cell cycle analysis

To further research the mechanism responsible for the anti-proliferative effect of compounds **9a** and **9b** in addition to enzyme inhibition assay, their apoptotic effects on SGC7901, PM8910 and A549 was evaluated. Compounds **9a** and **9b** were incubated in cultured cancer cells for 24 h and then analyzed in order to predict the phase of the cell cycle at which the growth of cells was inhibited. MTS data showed that **9a** had an IC_{50} of 9.75 μM on SGC7901, 6.74 μM on PM8910, and 10.13 μM on A549, and **9b** has an IC_{50} of 2.85 μM on SGC7901, 2.76 μM on PM8910, and 3.04 μM on A549, which are considered as suitable values of compound concentration for cell cycle analysis. Figure 2 shows the cell cycle analysis results obtained after treatment of SGC7901, PM8910 and A549 cells with **9a** or **9b** for 24 h (Gefitinib was used as a positive control). Inspection of the results showed that the cells have halted in the G1 phase and their transformation into the S phase has stopped relative to the negative control (Fig. 2). This implies the likelihood that c-Kit kinase was involved in the anti-proliferative activity of compounds **9a** and **9b**.

3.5. Docking study

In order to predict the possible binding mode of compounds **9a** and **9b** inside the binding site of c-Kit kinase, compounds were

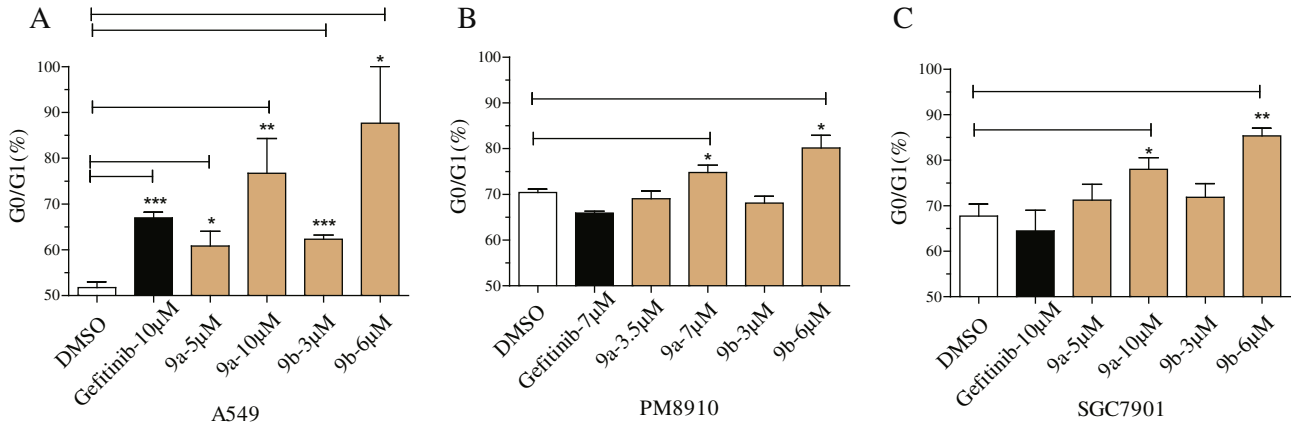

Figure 2. Cell cycle analysis of active compounds **9a** and **9b**. PM8910, SGC7901 and A549 cells were planted in 60 mm plates. In the following days, cells were treated with desired doses of **9a** and **9b** for 24 h. Cells were washed twice with PBS, fixed in ice-cold ethanol (75% vol/vol in water), and stained with the PI solution (25 mg/ml PI, 180U/ml RNase, 0.15%Triton X-100, and 30 mg/ml polyethylene glycol in 4 mmol/l citrate buffer, pH7.8; all from Sigma–Aldrich, St. Louis, MO) overnight at 4 °C. The results were presented as the percent of G0/G1 phase. Each bar represents mean ± SEM of three independent experiments. Statistical significance relative to DMSO group was indicated, $^{*}p < 0.05$, $^{**}p < 0.01$.

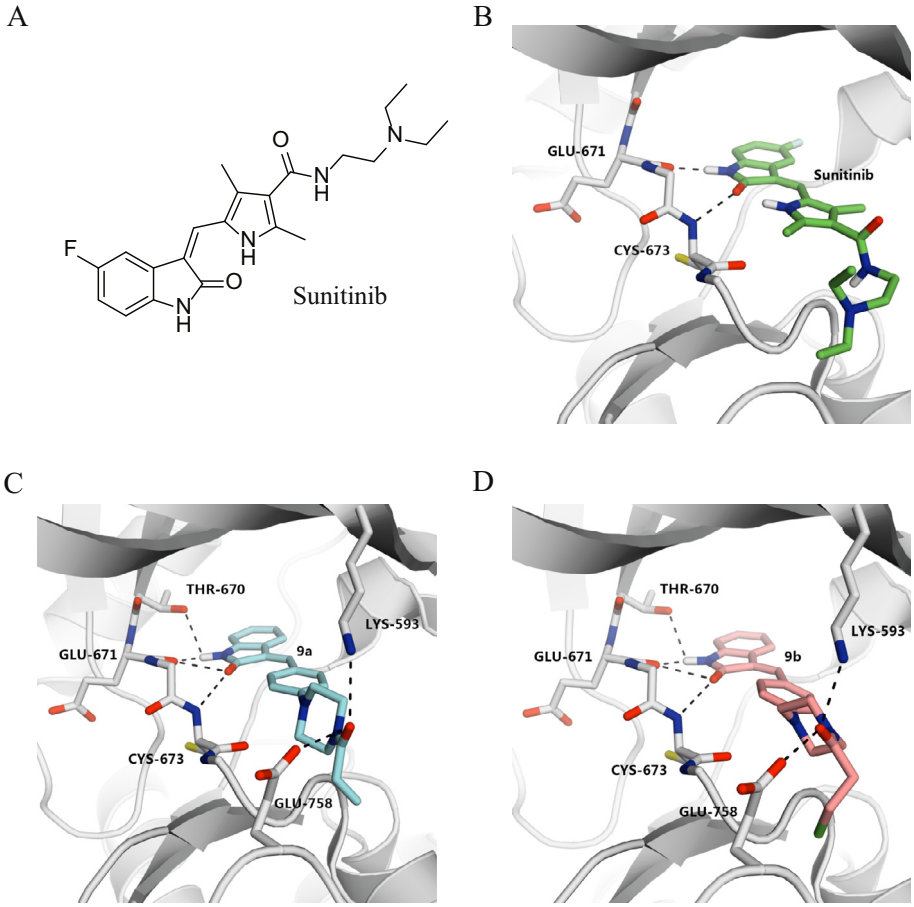

Figure 3. Chemical structure of c-Kit kinase inhibitor sunitinib (A) and Molecular docking simulation of sunitinib (B), compound **9a** (C) and **9b** (D) inside the ATP binding pocket of c-Kit enzyme.

docked into the ATP binding site of c-Kit kinase (PDB ID:3G0E) using Sybyl-2.0 software.

Sunitinib is an oxindole c-Kit kinase inhibitor developed by Pfizer (Fig. 3**A**). The cocrystallization of sunitinib fitting into the ATP binding site of c-Kit kinase indicated that the NH and O atoms of the sunitinib dihydroxyindole ring system make up the donor–acceptor motif that is frequently part of kinase inhibitors and participates in hydrogen-bonding interactions with the backbone amides in the interlobe hinge region of the protein. In detail, the O atoms on the oxindole ring does form hydrogen bond with Cys673, and the NH

atoms of the oxindole ring makes another hydrogen bond with Glu671 (Fig. 3B). Comparing the binding mode of **9a** and **9b** with the sunitinib illustrated that the oxindole moiety established hydrogen bonds with Glu671 and Cys673 of the hinge residue and form another hydrogen bond with Thr 670. In addition, the carbonyl of the piperazine form another two hydrogen bonds with Lys593 and Glu758 which make the chemical 9a and 9b inhibit the c-Kit kinase strongly (Fig. 3C and **D**). The docking of c-Kit kinase domain with all presented compounds was also performed. The docking scores of all compounds in c-Kit kinase domain were shown in Table S2. Based on the docking score, **9a** and **9b** are predicted as the two strongest c-Kit inhibitors among these compounds, which is consistent with the experimental data.

4. Conclusion

In summary, we synthesized several derivatives of indole-2-one and screened their anti-proliferative activities against nine human cancer cell lines. Several compounds showed significant suppression of the proliferation of the cancer cells. In particular, compounds **9a** and **9b** exhibited strong activity against many cancer cell lines and showed a broad spectrum of anticancer properties. Since **9a** and **9b** showed low inhibition of FGFR1, they were tested against five other kinases, and showed significant inhibition of receptor tyrosine kinase, c-Kit. In addition, evidence of kinase inhibition was implicated by cell cycle analysis as the **9a** and **9b** arrested the cell cycle in the G1 phase and the computer simulation also exhibited a positive result. Further studies should include detailed examination of the structure–activity relationship of these compounds, considering cell line inhibitions as well as the determination of the exact cellular targets of the interesting anti-proliferative compounds.

Acknowledgements

Financial support was provided by the National Natural Science Funding of China (21202124), High-level Innovative Talent Funding of Zhejiang Department of Health (G. L.), Project of Wenzhou Sci&Tech Bureau (Y20120061), Qianjiang Talent Project of Zhejiang Province (2013R10020), and Zhejiang Key Group Project in Scientific Innovation (2010R50042). We also kindly thank Professor S.H. Cheon in Chonnam National University for performing the molecular docking experiments.

Supplementary data

Supplementary data associated with this article can be found, in the online version, at http://dx.doi.org/10.1016/j.bmc.2014.10.017.

Reference

1. Sloane, D. *Methods Mol. Biol.* **2009**, *471*, 65.
2. Hotta, K.; Ueoka, H. *Crit. Rev. Oncol. Hematol.* **2005**, *55*, 45.
3. Szkudlinski, M. W. *Med. Hypotheses* **1992**, *39*, 265.
4. Rizzo, J.; Riley, C.; von Hoff, D.; Kuhn, J.; Phillips, J.; Brown, T. *J. Pharm. Biomed. Anal.* **1990**, *8*, 159.
5. Goseki, N.; Maruyama, M.; Nagai, K.; Kando, F.; Endo, M.; Shimoju, K.; Wada, Y. *Gan To Kagaku Ryoho* **1995**, *22*, 1028.
6. Fujita, J.; Tokuda, H.; Sugawara, K.; Yoshida, O. *Toxicol. Lett.* **1984**, *22*, 261.
7. Shoeb, M. *Bangladesh J. Pharmacol.* **2006**, *1*, 35.
8. Fujii, T.; Maeda, M. *Nihon Sanka Fujinka Gakkai Zasshi* **1988**, *40*, 593.
9. Zee-Cheng, R. K.; Cheng, C. C. *J. Med. Chem.* **1978**, *21*, 291.
10. Zee-Cheng, R. K.; Podrebarac, E. G.; Menon, C. S.; Cheng, C. C. *J. Med. Chem.* **1979**, *22*, 501.
11. Dancey, J.; Sausville, E. A. *Nat. Rev. Drug Discovery* **2003**, *2*, 296.
12. Cohen, P. *Nat. Rev. Drug Discovery* **2002**, *1*, 309.
13. Liang, G.; Liu, Z.; Wu, J.; Cai, Y.; Li, X. *Trends Pharmacol. Sci.* **2012**.
14. Li, E.; Hristova, K. *Biochemistry* **2006**, *45*, 6241.
15. Xu, A. M.; Huang, P. H. *Cancer Res.* **2010**, *70*, 3857.
16. Manning, G.; Whyte, D. B.; Martinez, R.; Hunter, T.; Sudarsanam, S. *Science* **2002**, *298*, 1912.
17. Liang, G.; Chen, G.; Wei, X.; Zhao, Y.; Li, X. *Cytokine Growth Factor Rev.* **2013**, *24*, 467.
18. Brooks, A. N.; Kilgour, E.; Smith, P. D. *Clin. Cancer Res.* **2012**, *18*, 1855.
19. Krug, M.; Hilgeroth, A. *Mini-Rev. Med. Chem.* **2008**, *8*, 1312.
20. Antoniu, S. A.; Kolb, M. R. *IDrugs* **2010**, *13*, 332.
21. Kuenen, B. C.; Giaccone, G.; Ruijter, R.; Kok, A.; Schalkwijk, C.; Hoekman, K.; Pinedo, H. M. *Clin. Cancer Res.* **2005**, *11*, 6240.
22. Mohammadi, M.; McMahon, G.; Sun, L.; Tang, C.; Hirth, P.; Yeh, B. K.; Hubbard, S. R.; Schlessinger, J. *Science* **1997**, *276*, 955.
23. Migliaccio, G.; Migliaccio, A. R.; Valinsky, J.; Langley, K.; Zsebo, K.; Visser, J. W.; Adamson, J. W. *Proc. Natl. Acad. Sci. U.S.A.* **1991**, *88*, 7420.
24. Tsai, M.; Takeishi, T.; Thompson, H.; Langley, K. E.; Zsebo, K. M.; Metcalfe, D. D.; Geissler, E. N.; Galli, S. J. *Proc. Natl. Acad. Sci. U.S.A.* **1991**, *88*, 6382.
25. Sanada, F.; Kim, J.; Czarna, A.; Chan, N. Y.; Signore, S.; Ogorek, B.; Isobe, K.; Wybieralska, E.; Borghetti, G.; Pesapane, A.; Sorrentino, A.; Mangano, E.; Cappetta, D.; Mangiaracina, C.; Ricciardi, M.; Cimini, M.; Ifedigbo, E.; Perrella, M. A.; Goichberg, P.; Choi, A. M.; Kajstura, J.; Hosoda, T.; Rota, M.; Anversa, P.; Leri, A. *Circ. Res.* **2014**, *114*, 41.
26. Krystal, G. W.; Carlson, P.; Litz, J. *Cancer Res.* **1997**, *57*, 2203.
27. Dos Santos, C.; McDonald, T.; Ho, Y. W.; Liu, H.; Lin, A.; Forman, S. J.; Kuo, Y. H.; Bhatia, R. *Blood* **2013**, *122*, 1900.
28. Mita, M.; Gordon, M.; Rosen, L.; Kapoor, N.; Choy, G.; Redkar, S.; Taverna, P.; Oganesian, A.; Sahai, A.; Azab, M.; Bristow, R.; Tolcher, A. W. *Cancer Chemother. Pharmacol.* **2014**, *74*, 195.
29. Gajiwala, K. S.; Wu, J. C.; Christensen, J.; Deshmukh, G. D.; Diehl, W.; DiNitto, J. P.; English, J. M.; Greig, M. J.; He, Y. A.; Jacques, S. L.; Lunney, E. A.; McTigue, M.; Molina, D.; Quenzer, T.; Wells, P. A.; Yu, X.; Zhang, Y.; Zou, A.; Emmett, M. R.; Marshall, A. G.; Zhang, H. M.; Demetri, G. D. *Proc. Natl. Acad. Sci. U.S.A.* **2009**, *106*, 1542.